SLAC-PUB-17
September 1963

INVESTIGATIONS OF TRAVELING-WAVE SEPARATORS FOR THE STANFORD TWO-MILE LINEAR ACCELERATOR*

O. H. Altenmueller, R. R. Larsen and G. A. Loew
Stanford Linear Accelerator Center
Stanford University, Stanford, California

(To be submitted to the Review of Scientific Instruments)

*Supported by the U. S. Atomic Energy Commission

ABSTRACT

Two traveling-wave rf structures, which are prototypes of devices to separate mass components of multi-BeV particle beams, have been designed and fabricated. Deflection characteristics have been studied by measuring the deflection of a 40 MeV electron beam.

I. INTRODUCTION

A. General Discussion

The idea of using rf fields to achieve mass separation of multi-BeV particles has received considerable attention in the past few years. Prompted by W.K.H. Panofsky's proposal,[1] several laboratories have engaged in investigations of the subject. The first experimental attempt to deflect high-energy particles with microwave fields was made by P. R. Phillips[2] at Stanford University. Programs to construct and use rf separators are presently underway at CERN (Geneva, Switzerland), Brookhaven National Laboratory (Upton, Long Island, New York), E.N.S. Orsay (Orsay, France), the Joint Institute for Nuclear Research (Dubna, USSR) and the Stanford Linear Accelerator Center (Stanford, California).

Mass separation with rf fields is a technique that will be particularly applicable to the time modulated secondary beams produced by the Stanford two-mile linear accelerator. The scheme is conceptually simple: the bunched electron beam hits a target and produces a bunched secondary beam which is then momentum analyzed. The distance between the target and the rf separator is adjusted so that the difference in time of flight between two mass components is one-half of the rf period. Hence, when they enter the separator, they experience equal but opposite deflecting forces. The klystron powering the separator can be of the same type as those used for acceleration and can be locked to the trigger and drive systems of the accelerator. By adjusting the phase of the separator, the particles can be made to "ride the crest" of the deflecting wave, thus undergoing maximum separation.

B. The Deflecting Mode

H. Hahn[3-7] of Brookhaven National Laboratory and Y. Garault[8-11] of Orsay, France have made extensive analytical studies of deflecting modes in iris-loaded cylindrical waveguides. By Fourier-analyzing the fields in an iris-loaded structure, Hahn and Garault obtain the following first order solution for the lowest order deflecting mode at $v_p = c$.

$$E_z = E_o \, kr \cos\theta \tag{1}$$

$$E_r = E_o \left[\left(\frac{kr}{2}\right)^2 + \left(\frac{ka}{2}\right)^2 \right] \cos\theta \tag{2}$$

$$E_\theta = E_o \left[\left(\frac{kr}{2}\right)^2 - \left(\frac{ka}{2}\right)^2 \right] \sin\theta \tag{3}$$

$$Z_o H_z = - E_o \, kr \sin\theta \tag{4}$$

$$Z_o H_r = - E_o \left[\left(\frac{kr}{2}\right)^2 - \left(\frac{ka}{2}\right)^2 + 1 \right] \sin\theta \tag{5}$$

$$Z_o H_\theta = E_o \left[\left(\frac{kr}{2}\right)^2 + \left(\frac{ka}{2}\right)^2 - 1 \right] \cos\theta \tag{6}$$

where k is the free-space wave number and a is the radius of the iris aperture (see Fig. 1a). From the Lorentz force on a particle of charge q, one obtains for the forces in rectangular coordinates

$$F_y = 0 \tag{7}$$

$$F_x = qE_o \tag{8}$$

Hence, the equivalent transverse deflecting field is uniform in magnitude and direction over the aperture. This property is desirable since it implies that one can expect an aberration-free deflection from this mode. Integrating the

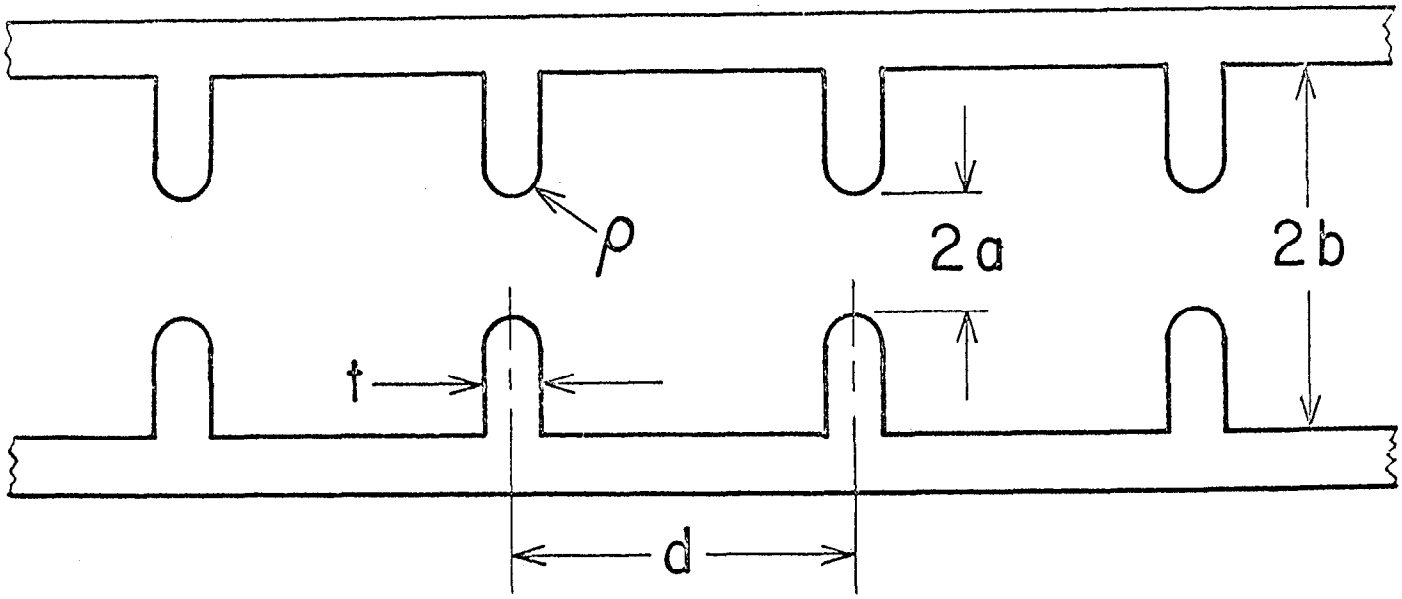

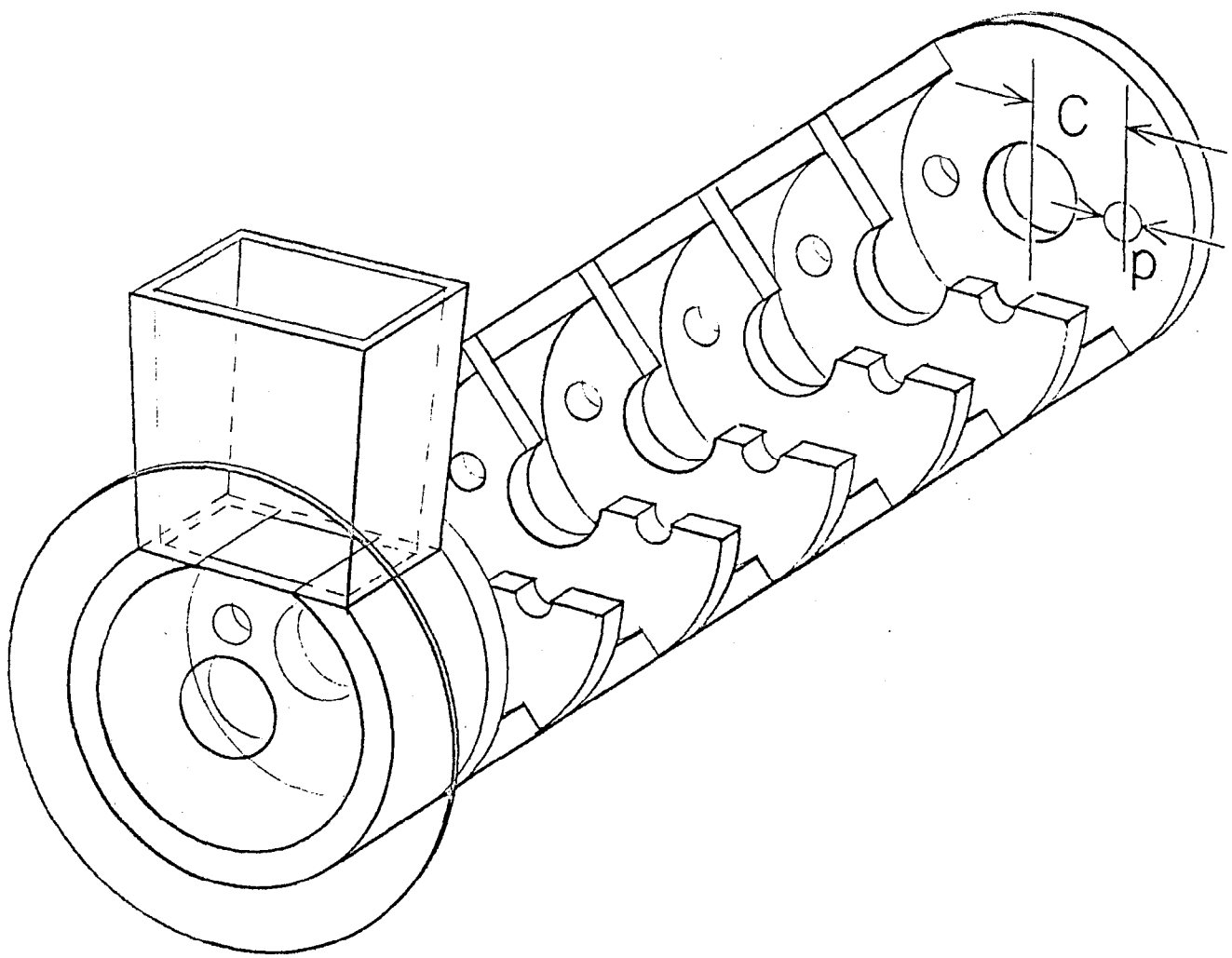

FIG. 1a--Schematic drawing of disk-loaded waveguide: modular dimensions of cavities.

FIG. 1b--Schematic drawing of disk-loaded waveguide: disks with suppressor holes.

Poynting vector over the aperture, one obtains for the power in the z direction

$$P_z = \frac{\pi a^2}{2} \frac{E_o^2}{Z_o} \left(\frac{ka}{2}\right)^2 \left[\frac{4}{3}\left(\frac{ka}{2}\right)^2 - 1\right] \tag{9}$$

From this expression one can estimate the deflecting field per unit power input. One observes that this deflecting mode is a forward or a backward wave mode depending on whether $ka > \sqrt{3}$ or $ka < \sqrt{3}$. For 2856 Mc/sec, the cross-over value of a is 2.9 cm.

An important criterion in the design of an rf separator is the optimization of the acceptance per unit power. This is a sensitive function of the separator dimensions and will not be discussed here. This paper reports the fabrication and testing of two prototype separators, Lola I and Lola II.

II. COLD TESTS AND FABRICATION OF RF STRUCTURE

A. Cold Tests

Two experimental models were designed and fabricated for testing on the Stanford Mark IV accelerator. Model Lola I is a conventional circularly symmetrical disk-loaded waveguide as shown in Fig. 1a. Model Lola II uses so-called "suppressor holes" as shown in Fig. 1b to prevent rotation of the deflecting plane caused by possible nonuniformities of the structure.

These empirical designs were obtained by means of conventional microwave techniques[12,13] using stacks of cylinders and disks. Table I outlines the physical dimensions and cold-test results. The cold-test frequency was adjusted to yield an operating frequency compatible with the operating frequency of the Mark IV accelerator (2857.250 Mc/sec).

TABLE I

PHYSICAL DIMENSIONS AND COLD-TEST RESULTS FOR

RF SEPARATORS LOLA I AND LOLA II

Designation	Symbol	Lola I	Lola II
Length in cavities	ℓ	13 cavities and 2 couplers	13 cavities and 2 couplers
Periodic length	d	3.5 cm	3.5 cm
Phase shift per cavity		$2\pi/3$	$2\pi/3$
Inside cavity diameter	2b	11.8542 cm	11.7894 cm
Iris diameter	2a	4.064 cm	4.064 cm
Iris aperture radius	ρ	0.3086 cm	0.3086 cm
Disk thickness	t	0.584 cm	0.584 cm
Suppressor hole diameter	p		1.905 cm
Suppressor hole radial distance	c		3.620 cm
Inside coupler diameter	$2b_{CPL}$	11.659 cm	11.659 cm
Terminal cut-off hole diameter		3.3 cm	3.6 cm
Thickness of cut-off disks		4.762 cm	3.8 cm
Cold-test frequency at 78°F and 42% relative humidity	f	2857.680 Mc/sec	2857.680 Mc/sec
Quality factor	Q	10700	9030
Relative group velocity	v_g/c	- 0.0311	- 0.0296
Attenuation	$I\ell$	0.047 nepers	0.058 nepers

Figure 2 gives the respective Brillouin or ω-β diagrams for structures very close in dimensions to Lola I and Lola II. It is important to notice how the 90° rotation of the axis of the suppressor holes with respect to the exciting probes causes the ω-β diagrams to be separated. Hence, by aligning the suppressor holes at 90° with the couplers as shown in Fig. 1b, mode rotation should be entirely prevented.

B. Fabrication of Lola I and Lola II

Both structures were built by brazing stacks of machined OFHC copper cylinders and disks. The brazing operation was carried out in four steps. First, the coupler cavities were furnace brazed. Their matching irises were then machined and checked for a rough match. Subsequently, two half stacks of six and seven cavities were brazed to the couplers. Both these operations were done with Nicoro at 1030°C. Next, the rectangular waveguide transitions were brazed onto the couplers using 50% copper-50% gold at 970°C. The last braze to join the two half-stacks was done using CuSil at 780°C. The vacuum flanges were heliarced, and the water cooling pipes were soft-soldered onto the wall of the structure. For Lola II, stainless steel mandrels were used to align the suppressor holes.

C. Matching of the Structures

After fabrication, both structures were submitted to a series of rf cold tests. These tests resemble closely those used to match and tune linear accelerator structures[12,13] and will not be described here. Machining and assembling tolerances were such that all cavity phase shifts came within ±5° of 120°, and no individual cavity tuning was deemed necessary. The coupling irises were matched using the nodal shift technique, both with a detuning plunger (1.27 cm in diameter) inserted into the structure and a sliding

short in the output waveguide. Contrary to expectations, plungers of larger diameters did not give satisfactory results.

The final VSWR into and out of the structures, including two ceramic vacuum windows, was of the order of 1.1:1.0. The input and output couplers have opposite orientations. This was done to cancel any possible spurious deflection caused by the field asymmetry due to the iris opening.

III. PERFORMANCE OF RF SEPARATOR MODELS

A. General Description of Experiment

Several experiments were performed to measure directly the deflection capability of the structures described. A schematic of the experimental arrangement is shown in Fig. 3. The electron beam of the 100-MeV Stanford Mark IV linear accelerator was momentum analyzed and transmitted through the separator. As the magnitude and phase of the microwave fields in the separator were varied, the motion of the electron beam in the horizontal plane was observed on a ZnS screen mounted on the end of a 2-meter evacuated drift tube that followed the separator.

B. Microwave System

Referring again to Fig. 3, it can be seen how the overall layout of the Mark IV accelerator was used to power the rf separator and to test its deflection properties. Of the two klystrons available in the machine, a fraction of the output of the second tube was coupled off the main waveguide feeding the second accelerator section by means of a 7 db directional coupler. Independent power level and phase control were achieved by means of a manually

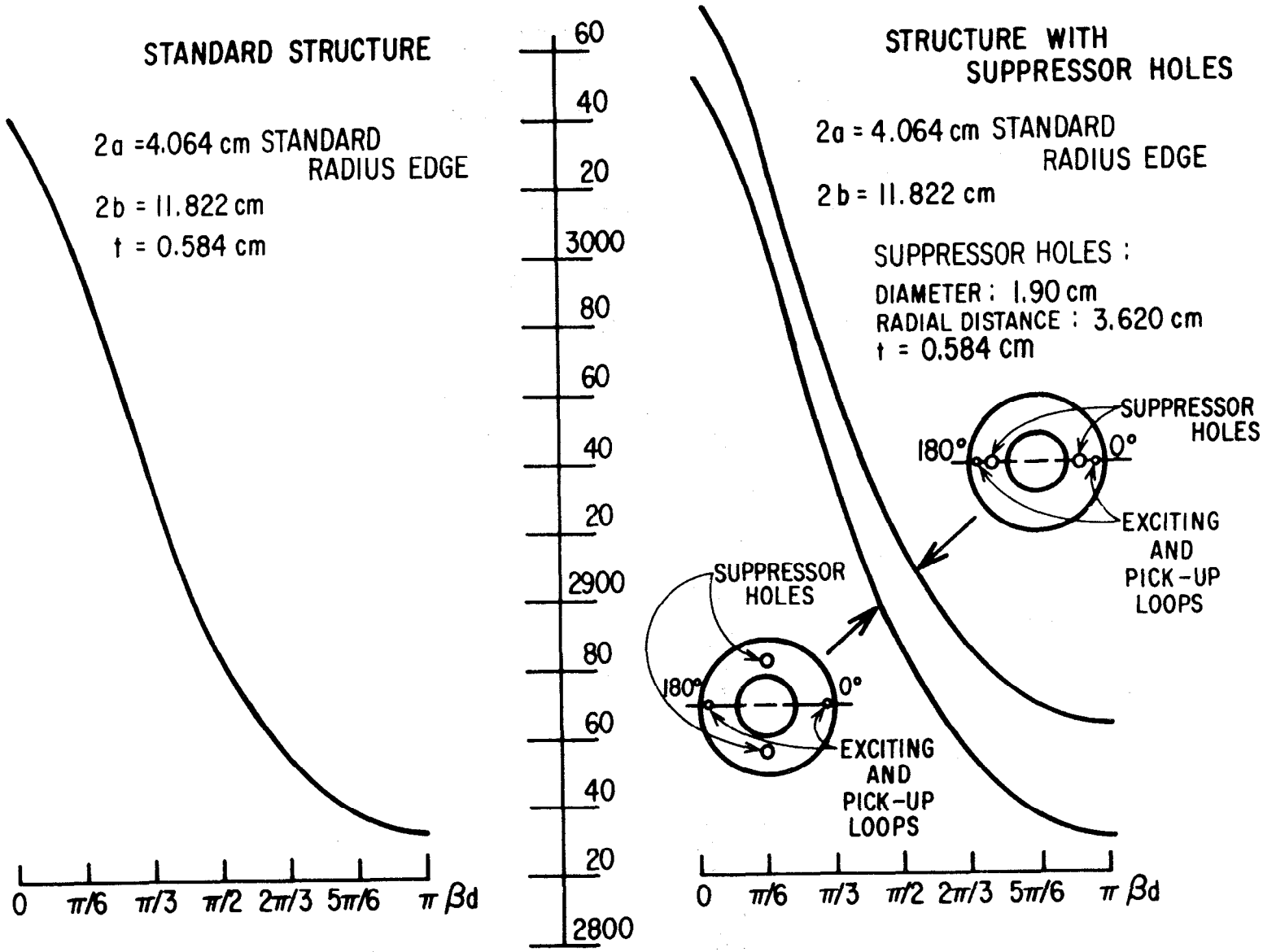

FIG. 2--ω-β diagrams for two rf separator designs; a. Standard structure; b. Structure with suppressor holes.

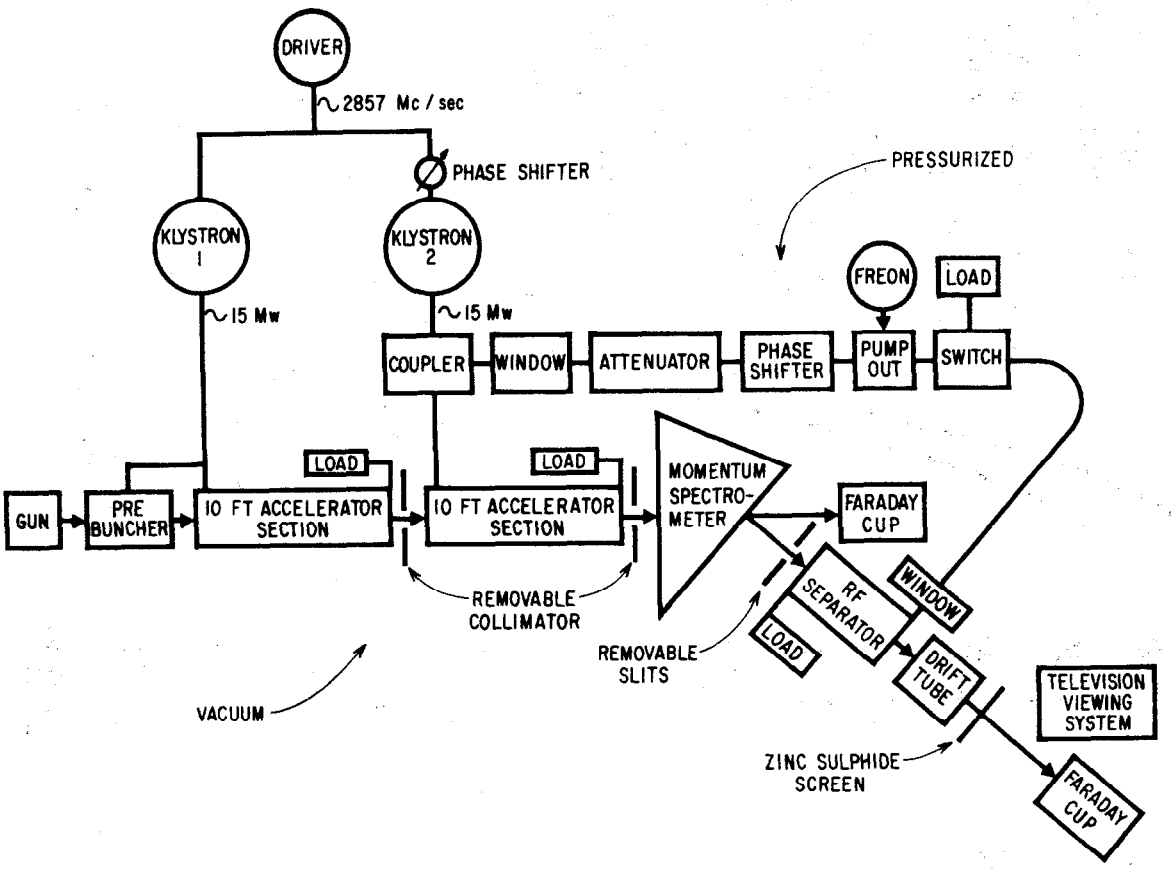

FIG. 3--Mark IV layout showing two accelerator sections with respective klystrons and rf separator with microwave circuitry.

driven attenuator and a motor driven trombone-type phase shifter. Following the phase shifter, a high power switch enabled one to transmit the microwave power to the rf separator or to dissipate it into a matched high power load. Input and output rf power levels were monitored by means of directional couplers (52.8 db and 52.4 db) and standard bolometer power bridges. The output of the separator looked into a pressurized matched load. The complete rf assembly from the 7 db directional coupler to the separator was isolated from the accelerator vacuum system by means of two ceramic windows, and it was pressurized to 30 pounds of Freon.

C. Electron Beam

The energy of the electron beams was varied over a range of 30 to 50 MeV ($\pm \approx 1\%$). This energy range permitted easily observable deflections and stable operation of the accelerator. For a given power output of the klystrons, the beam transmitted through the momentum analyzing slits (monitored by the Faraday cup and the ZnS screen) was optimized by varying the current in the wedge-shaped analyzing magnet (30° bend). An analyzed beam current of 1 mμamp was easily observed on the screen.

The removable collimators at the end of each accelerator section and the width of the momentum slits made it possible to vary the beam cross section from 2.5 × 2.5 cm to 0.5 × 0.5 cm. By varying the strength of a steering dipole located at the beginning of the second accelerator section, it was possible to translate the beam relative to the axis of the separator by as much as ±1 cm in the vertical plane. The phase-bite of the electron beam was varied by making small changes in the operating frequency of the accelerator above 2857.3 Mc/sec. The entire system, from accelerator gun to ZnS screen, was evacuated to avoid multiple-scattering of the beam.

D. Experimental Results

1. Deflection Versus Phase

At a constant power level and beam momentum, the beam deflection was measured as a function of the relative phase of the fields in the separator with respect to the electron beam bunches. The results are shown in Fig. 4 where the abscissa is in units of linear displacement of the phase shifter. The data traces out a sine curve. This data was obtained for Lola I. For this measurement and for all subsequent ones, the deflection was measured to an accuracy of ± 1 mm.

2. Effect of Size of Phase Interval

By increasing the frequency above the normal operating frequency of the accelerator, the accelerated bunch width was increased. This resulted in a broadening of the spot size. The effect is most noticeable as one passes through the region of zero deflection, for it is in this region that the fields are changing most rapidly with phase.

3. Deflection Versus Power

By adjusting the attenuator to the separator, it was possible to vary the power into the separators without changing the energy of the electron beam. At all given power levels, the maximum obtainable deflection (as a function of phase) was measured. Figure 5 shows the maximum deflection as a function of the square root of the peak power in the structures. The abscissa is proportional to the average of the peak deflecting field for negligible attenuation. An uncertainty of ±10 percent must be assigned to the power measurement, due primarily to the uncertainty in the input and output coupling ratios and the power meters. This uncertainty dominates the uncertainty in the value of the deflection. From the slope of the lines in Fig. 5 and a knowledge of the beam momentum and experimental geometry, the

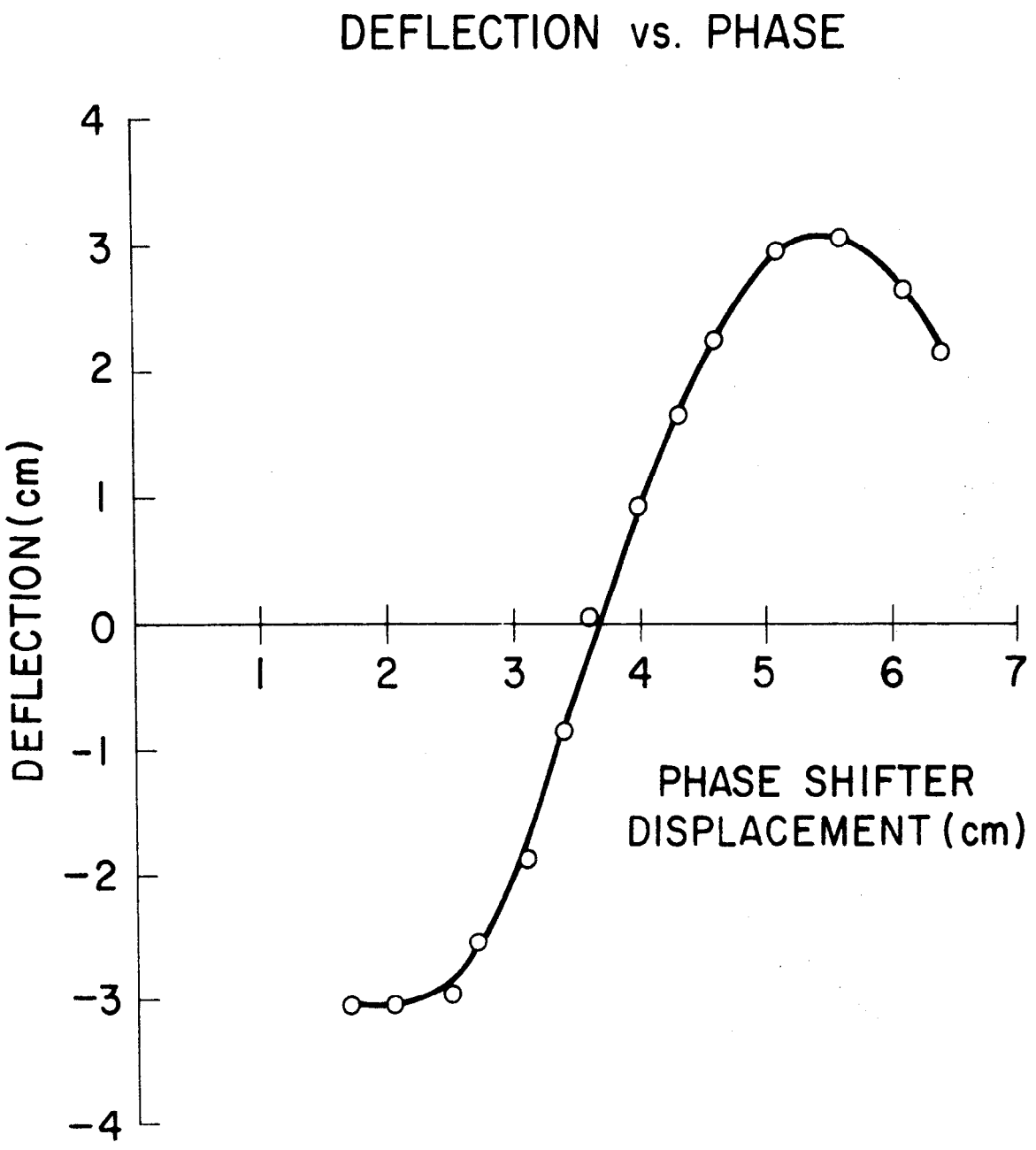

FIG. 4--Deflection vs phase.

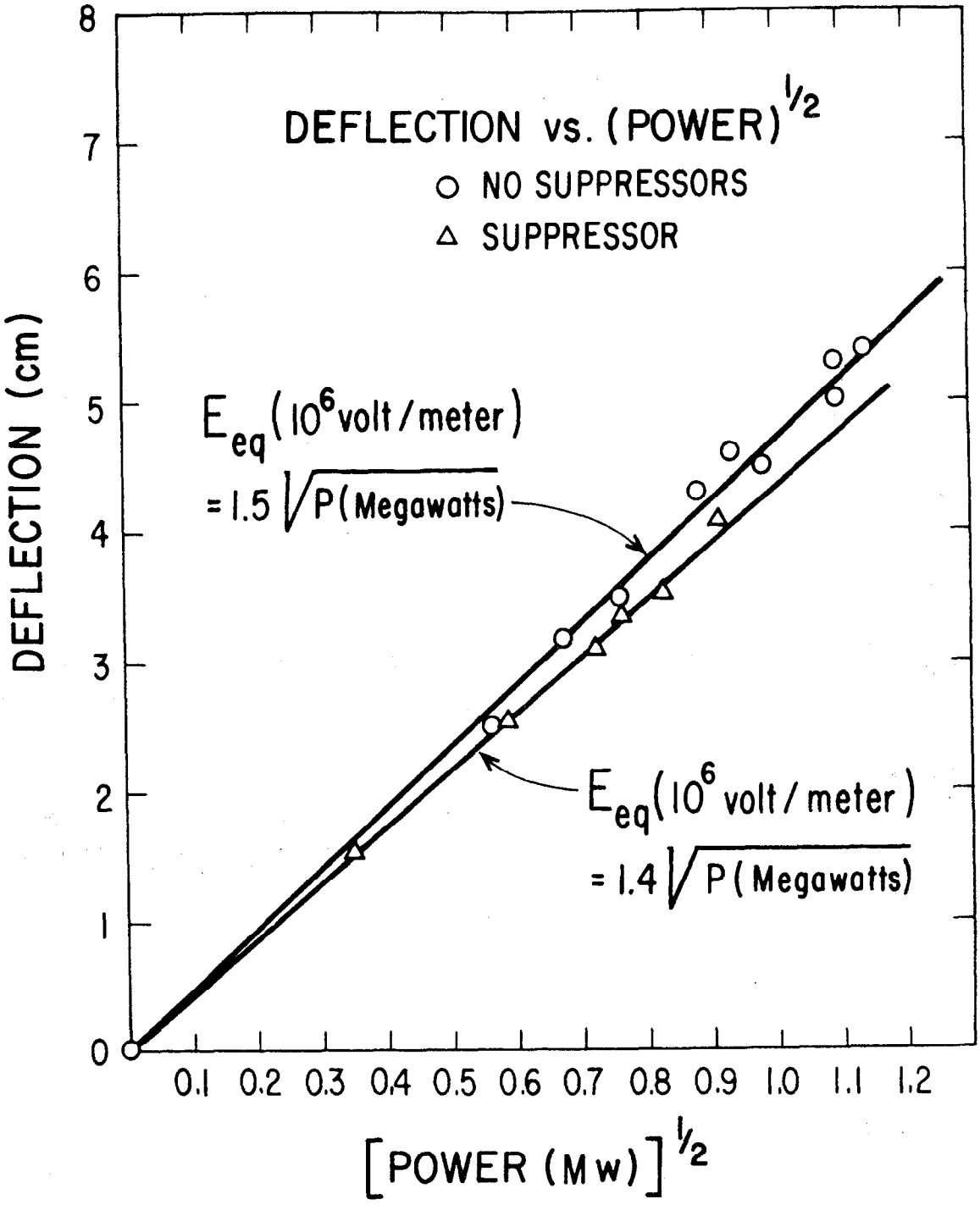

FIG. 5--Deflection vs $(\text{power})^{1/2}$.

relation between the equivalent deflecting field strength and the power can be deduced:

$$E_{eq}(10^6 \text{ volt/meter}) = 1.5\sqrt{P(\text{Megawatts})} \tag{10}$$

for Lola I and

$$E_{eq}(10^6 \text{ volt/meter}) = 1.4\sqrt{P(\text{Megawatts})} \tag{11}$$

for Lola II. The uncertainties are of the order of ±5%.

4. Uniformity of Deflecting Field

By collimating the beam at the output of the first accelerator section and by activating the steering dipole at the beginning of the second section, a vertical transverse momentum was imparted to the electron beam. This resulted in a ±1.25 cm vertical excursion of the beam at the ZnS screen and, considering the geometry of the experimental arrangement, a ±1 cm excursion at the separator. Figure 6 shows that the maximum obtainable deflection of the beam is unchanged under these conditions. Both structures exhibited this behavior. It was impractical to explore the field uniformity near the disk edges.

IV. COMPARISON OF THEORY AND EXPERIMENT

H. Hahn has introduced the dimensions of our structure into his computer program and calculated some of its properties. He obtained a relative group velocity of - 0.031, in good agreement with cold-test measurements. However,

the calculation of $E_{eq} = 1.78\sqrt{P}$ is higher than the measured value. In view of the complexity of the problem, the agreement between experiment and theory can be considered to be reasonably good. On the basis of the results obtained, it can be concluded that traveling-wave structures supporting this "TM_{11}-like" or HEM_{11} mode can be used as mass separators at multi-BeV energies.

Before adopting a final design for the two-mile accelerator, several parameters such as optimum group velocity, number of disks per wavelength, method of mode rotation suppression, resulting shunt impedance, etc., need to be investigated in greater detail. These activities will soon be undertaken at SLAC; the first step, presently underway, will be to build a model with a relative group velocity of - 0.007.

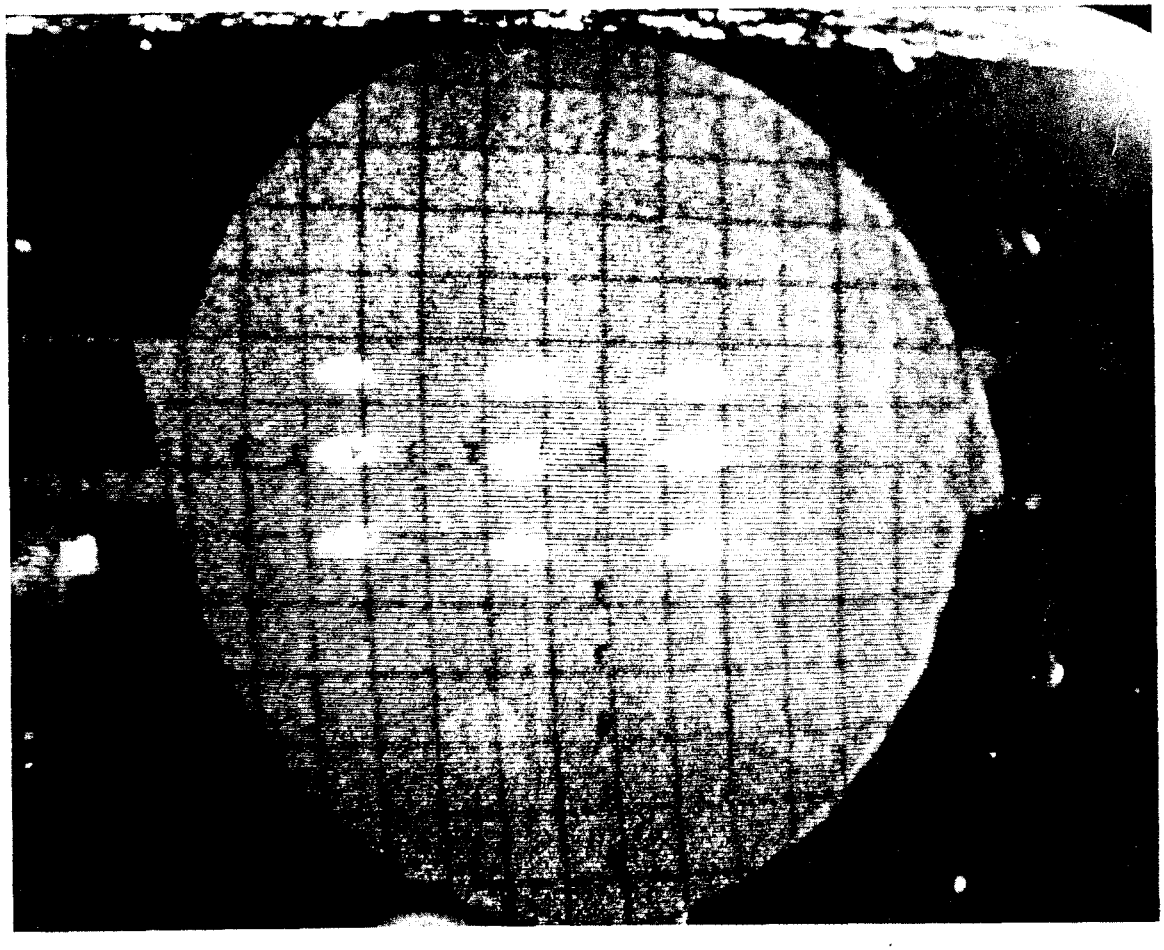

FIG. 6--Beam spots on ZnS screen for zero and extreme deflections at three different vertical positions.

LIST OF REFERENCES

1. W.K.H. Panofsky, "A Mass Sensitive Deflector for High Energy Particles," HEPL-82 (Internal Memo), High Energy Physics Laboratory, Stanford University, Stanford, California (May 1956).
2. P. R. Phillips, "The Separation of High-Energy Particle Beams by Microwave Techniques," Ph.D. Thesis, Department of Physics, Stanford University, Stanford, California (November 1960).
3. H. Hahn, "The Deflecting Mode in the Circular Iris-Loaded Waveguide of an RF Particle Separator," Internal Report BNL-AGS HH-5, Brookhaven National Laboratory, New York (1962).
4. H. Hahn, "Longitudinal Electromagnetic Modes in Circular Cylinder Coordinates," Internal Report, Brookhaven National Laboratory HH-4, New York (May 1962).
5. H. Hahn, "The Brookhaven RF Particle Separator," Minutes BNL-CERN Meeting, Brookhaven National Laboratory, New York; p. 103 (1962).
6. H. Hahn, "Space Harmonic Analysis of the $\pi/2$ Deflecting Mode: The Maximum Deflection," BNL-AGS Report HH-6, Brookhaven National Laboratory, New York (April 1963).
7. H. Hahn and H. J. Halama, "Mode Identification in the Iris-Loaded Waveguide of an RF Particle Separator," AGS Internal Report HH/HJH-2, Brookhaven National Laboratory, New York (January 1963).
8. Yves Garault, "Electromagnetic Waves of the E.H. Type in a Circular Waveguide with Metallic Irises," Comptes Rendus, Paris, Vol. 255, p. 2920 (1962).
9. Yves Garault, "Propriétés générales d'un type d'ondes utilisables dans les accélérateurs pour les deflecteurs h.f. de particules rapides," GT/62-1, Orsay, France (1962).

10. Yves Garault, "Ondes EH du guide cylindrique circulaire chargé par des iris métalliques," GT/62-2, Orsay, France (1962).

11. Yves Garault, "Étude des lignes de force du champ électromagnétique du mode EH_{11} déflecteur du guide à iris," GT/62-3, Orsay, France (1962).

12. E. L. Ginzton, Microwave Measurements, McGraw-Hill Book Company, Inc., New York (1957).

13. A. L. Eldredge, G. A. Loew and R. B. Neal, "Design and Fabrication of the Accelerating Structure for the Stanford Two-Mile Accelerator," SLAC Report No. 7, Stanford Linear Accelerator Center, Stanford University, Stanford, California (1962).